

## Supplementary Information

### Dual enhancement in strength and ductility of Fe-rich medium-entropy alloys via in-situ formed heterogeneous multi-phase structure

Jian Wu<sup>a, 1</sup>, Xinghua Zhu<sup>b, 1</sup>, Sirui, Huang<sup>a</sup>, Heguo Zhu<sup>a, \*</sup>

*a* College of Materials Science and Engineering, Nanjing University of Science and Technology, Nanjing 210094,

*PR* China

*b* Key Laboratory of Advanced Technologies of Materials, Ministry of Education, School of Materials Science and

Engineering, Southwest Jiaotong University, Chengdu, 610031, China

---

<sup>1</sup> These authors contributed equally to this work.

\* Corresponding author. E-mail address: [zhg1200@njust.edu.cn](mailto:zhg1200@njust.edu.cn) (H.G. Zhu)

Microstructural evolutions of  $\text{Ni}_{0.6}\text{CoFe}_{1.4}\text{Si}_x$  MEAs caused by addition of Si are given in Fig. S1. Si0 alloy exhibits a uniform single-phase feature, which is determined as the BCC phase based on the XRD observations. As shown in Figs. S1b-d, after adding Si in the base alloy, the Si-containing alloys (Si0.1, Si0.2 and Si0.3) show a typical dendrite (DR) structure. Meanwhile, some granular precipitates can be detected in the inter-dendrite (ID) regions, and the size of precipitates in Si0.1 Si0.2 and Si0.3 alloys is 2.02, 2.67 and 3.37  $\mu\text{m}$ , respectively. Fig. S1e is the EDS elemental distribution of Si0.3 alloy, in which the granular precipitates are rich in Ni and Si elements. The result is consistent with the study of Huang et al.<sup>1</sup> Additionally, the EDS point analysis is utilized to determine the elemental compositions of DR region, IR region and precipitates (marked as P) in  $\text{Ni}_{0.6}\text{CoFe}_{1.4}\text{Si}_x$  MEAs, and the corresponding results are shown in Table S1. The Si content is slightly higher in the IR regions than that in the DR regions. Similar result has been revealed in previous study.<sup>2</sup> The element segregation in these alloys results from the different mixing enthalpy value of Si with other constituent elements.<sup>3</sup> Moreover, the atomic ratio of Ni and Si elements in the granular precipitates is close to 1:1, suggesting that the particle is the NiSi typed phase.

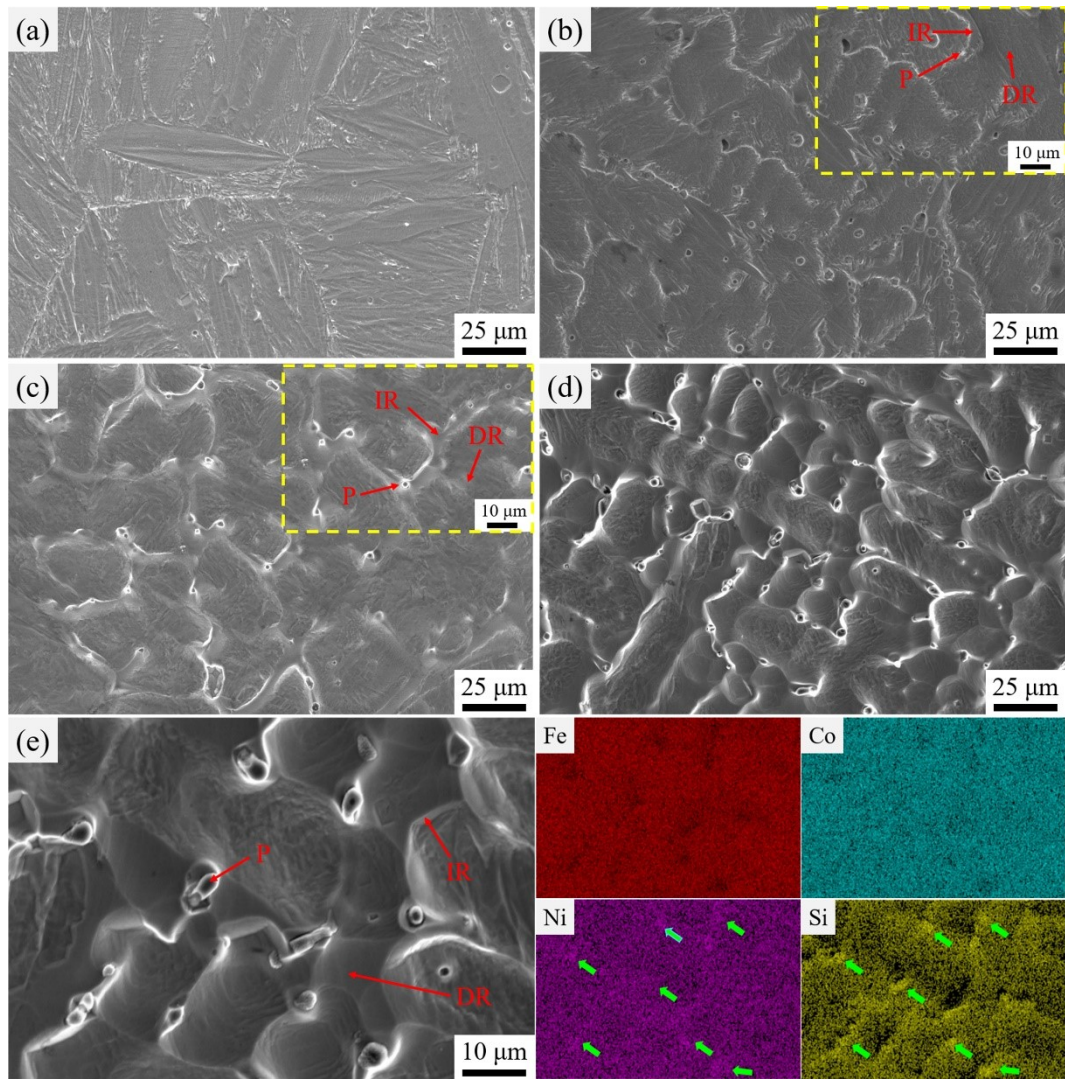


Fig. S1. SEM images of  $\text{Ni}_{0.6}\text{CoFe}_{1.4}\text{Si}_x$  MEAs: (a)  $\text{Si}_0$ , (b)  $\text{Si}_{0.1}$ , (c)  $\text{Si}_{0.2}$  and (d)  $\text{Si}_{0.3}$ ; (e) Enlarged images and corresponding EDS maps of  $\text{Si}_{0.3}$  alloy. Inset in (b) and (c) are the magnified SEM images of the  $\text{Si}_{0.1}$  and  $\text{Si}_{0.2}$  alloys, respectively.

Table S1. EDS analysis results of the different regions in the  $\text{Ni}_{10.6}\text{CoFe}_{1.4}\text{Si}_x$  MEAs.

Alloys	Regions	Elements (at.%)			
		Fe	Co	Ni	Si
Si0.1	DR	46.4	32.3	18.2	3.2
	IR	42.4	30.1	20.1	7.4
	P	43.6	27.7	16.2	12.5
Si0.2	DR	45.8	30.6	17.7	5.9
	IR	40.5	30.6	21.8	7.0
	P	21.1	20.0	31.4	26.5
Si0.3	DR	42.8	30.5	17.7	9.0
	IR	41.6	29.6	17.6	11.2
	P	22.4	21.7	28.3	27.6

Fig. S2 shows the variation of KAM value with strain. The KAM value is firstly increased and then decreased with increasing the strain.

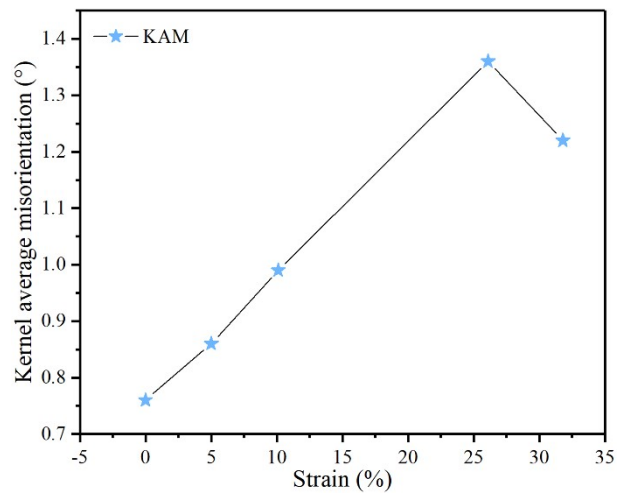


Fig. S2. Variation of KAM value with strain.

The detailed information of the current Si0.3 alloy and other reported H/MEAs is shown listed in Table S2. Interestingly, Si0.3 alloy exhibit an excellent strength-ductility combination as compared to the other alloys.<sup>4-12</sup>

Table S2. Mechanical properties of the typical H/MEAs at room temperature.

Alloys	YS (MPa)	UTS (MPa)	FE (%)	References
FeCrMnVSi <sub>0.5</sub>	211	762	18	[4]
FeCrMnVSi <sub>1.0</sub>	199	767	16	[4]
FeCrMnVSi <sub>1.5</sub>	262	834	17	[4]
FeCrMnVSi <sub>2.0</sub>	216	1071	19	[4]
FeMnNiSi <sub>0.005</sub>	197	493	59.11	[5]
FeMnNiSi <sub>0.01</sub>	220	508	68.59	[5]
FeMnNiSi <sub>0.02</sub>	249	528	70.01	[5]
Fe <sub>35</sub> Mn <sub>25</sub> Al <sub>15</sub> Cr <sub>5</sub> Ni <sub>15</sub> C <sub>5</sub>	-	855	2.5	[6]
CrFeNiAl <sub>0.27</sub> Si <sub>0.11</sub> Mo <sub>0.02</sub>	577.1 ± 10.0	1011.3 ± 12.1	15.5 ± 0.6	[7]
CrFeNiAl <sub>0.28</sub> Si <sub>0.12</sub>	656 ± 16	1133 ± 32	8.1 ± 1.7	[8]
Fe <sub>2</sub> CrNiSi <sub>0.3</sub> Al <sub>0.28</sub>	633 ± 49	1259 ± 42	9.32 ± 0.18	[9]
FeCrVTiSi <sub>0.5</sub>	238	774	17.7	[10]
FeCrVTiSi <sub>1.0</sub>	303	898	17.9	[10]
FeCrVTiSi <sub>1.5</sub>	318	933	18.7	[10]
FeCrVTiSi <sub>2.0</sub>	210	604	10.8	[10]
Al <sub>0.3</sub> CoCrFeNiSi <sub>0.1</sub>	217 ± 6.1	489 ± 9.5	98 ± 1.2	[11]
Al <sub>0.3</sub> CoCrFeNiSi <sub>0.2</sub>	258 ± 3.5	591 ± 11.1	86 ± 2.5	[11]

$\text{Al}_{0.3}\text{CoCrFeNiSi}_{0.3}$	$428 \pm 9.2$	$717 \pm 16.0$	$58 \pm 1.1$	[11]
$(\text{Fe}_{50}\text{Mn}_{30}\text{Co}_{10}\text{Cr}_{10})_{96}\text{Si}_4$	299	749	34.3	[12]
$(\text{Fe}_{50}\text{Mn}_{30}\text{Co}_{10}\text{Cr}_{10})_{92}\text{Si}_8$	312	831	27.4	[12]
$(\text{Fe}_{50}\text{Mn}_{30}\text{Co}_{10}\text{Cr}_{10})_{88}\text{Si}_{12}$	309	866	25.8	[12]
$\text{Ni}_{0.6}\text{CoFe}_{1.4}\text{Si}_{0.3}$	$669.5 \pm 19.9$	$1096.9 \pm 39.0$	$31.7 \pm 0.3\%$	This work

The cost comparison of the Si0.3 and other alloys are listed in Table S3. The cost of Si0.3 alloy for the same 1kg is lower than that of the other H/MEAs.<sup>13</sup> Therefore, low-cost and high-performance Si0.3 alloy has more advantages in industrial applications.

Table S3. Cost comparison of Si0.3 and other alloys.

Alloys	Price (\$/kg)	References
AlCoCrCuNiTiY	26.5	[13]
AlCoCuFeNiZr	33.8	[13]
CoFeMnTiVZr	35.2	[13]
CoCrFeMoNiVZr	33.1	[13]
AgAlCoCuFeCoCu	164.7	[13]
AlNbTiVZr	40.8	[13]
$\text{Ni}_{0.6}\text{CoFe}_{1.4}\text{Si}_{0.3}$	17.8	This work

## References

1. L. Huang, X. Wang, F. Jia, X. Zhao, B. Huang, J. Ma and C. Wang, *Mater. Lett.*, 2021, **282**, 128809.
2. X. Gao, Y. Chen, R. Chen, T. Liu, H. Fang, G. Qin, Y. Su and J. Guo, *Intermetallics.*, 2022, **147**, 107617.
3. J. Lu, Y. Weng, A. Wan, X. Sui, J. Hu and C. Huang, *J. Therm. Spray. Techn.*, 2023, **32**, 2250-2261.
4. Y. Liu, Z. Yao, P. Zhang, S. Lin, M. He, S. Lu and X. Wu, *Mater. Design.*, 2023, **225**, 111565.
5. S. R. Jha, J. Sen, J. Kumar and K. Biswas, *J. Alloy. Compd.*, 2023, **965**, 171491.
6. C. Hu, J. Zhang, Y. Zhang, K. Han, C. Li, C. Song and Q. Zhai, *J. Iron. Steel. Res. Int.*, 2018, **25**, 877-882.
7. X. Li, X. Liu, N. Lei, G. Zhang, R. Wei, T. Wang, S. Wu, Y. Cai, S. Guan, F. Li and C. Chen, *Mater. Today. Commun.*, 2023, **35**, 106020.
8. C. Chen, S. Yuan, X. Li, J. Chen, W. Wang, R. Wei, T. Wang, T. Zhang, S. Wu, S. Guan and F. Li, *Mater. Today. Commun.*, 2023, **35**, 105523.
9. N. Lei, G. Zhang, X. Li, S. Wu, T. Wang, Y. Cai, R. Wei, S. Guan, F. Li and C. Chen, *Mater. Lett.*, 2023, **344**, 134447.
10. S. Lin, Y. Yao, Z. Yao, G. Shi, Y. Liu, P. Zhang, S. Lu, W. Qin and X. Wu, *Surf. Coat. Tech.*, 2024, **484**, 130872.
11. X. Gu, Y. Zhuang and P. Jia, *Mat. Sci. Eng. A-Struct.*, 2022, **840**, 142983.
12. H. Jiao, W. Wu, Z. Hou, Y. Tang, Y. Hu, D. Liu and L. Zhao, *Mater. Today.*



*Commun.*, 2024, **38**, 107694.

13. X. Fu, C. A. Schuh and E. A. Olivetti, *Scripta. Mater.*, 2017, **138**, 145-150.